Journal of Molecular Catalysis A: Chemical 342–343 (2011) 58–66

Contents lists available at ScienceDirect

Journal of Molecular Catalysis A: Chemical

journal homepage: www.elsevier.com/locate/molcata

Palladium complex catalysts immobilized on silica via a tripodal linker unit with amino groups: Preparation, characterization, and application to the Suzuki–Miyaura coupling

Norihisa Fukaya[a], Masae Ueda[a], Syun-ya Onozawa[a,*], Kyoko K. Bando[a], Takayuki Miyaji[b], Yukio Takagi[b], Toshiyasu Sakakura[a], Hiroyuki Yasuda[a,*]

[a] National Institute of Advanced Industrial Science and Technology (AIST), Tsukuba Central 5, 1-1-1 Higashi, Tsukuba, Ibaraki 305-8565, Japan
[b] N.E. CHEMCAT Corporation, 678 Ipponmatsu, Numazu, Shizuoka 410-0314, Japan

ARTICLE INFO

Article history:
Received 25 February 2011
Received in revised form 7 April 2011
Accepted 7 April 2011
Available online 22 April 2011

Keywords:
C–C coupling
Suzuki–Miyaura reaction
Immobilized catalyst
Amino-functionalized silica
Palladium

ABSTRACT

To clarify the effectiveness of a tripodal linker unit (3-bromopropyltris[3-(dimethylisopropoxysilyl)propyl]silane), which can be bound to a silica surface via three independent Si–O–Si bonds, silica-immobilized palladium amine complex catalysts employing the tripodal linker unit were prepared and applied toward the Suzuki–Miyaura coupling reaction. *N*-Functionalized (*N* = 3-methylaminopropyl, 3-dimethylaminopropyl, or *N*,*N*-dimethylethylenediaminopropyl) silica materials were prepared by grafting the tripodal linker unit onto mesoporous silica followed by treatment with the corresponding amine. A series of silica-immobilized amino-palladium complex catalysts were prepared by reacting *N*-functionalized silica materials with palladium acetate. A catalyst that included a methylamino ligand and a ligand-to-Pd molar ratio of 6:1 gave the best performance for the reaction between aryl bromides and phenylboronic acid in toluene. Moreover, catalysts containing the tripodal linker showed lower levels of palladium leaching after the reaction and better recyclability compared to catalysts having conventional trialkoxy-type linkers.

1. Introduction

Immobilization of molecular catalysts via linkers on inorganic oxide supports, for example, the tethering of metal complex catalysts by propylene chains to silica, is a promising strategy for facilitating the separation of catalysts from reaction mixtures and for assisting the catalyst recycling process [1–5]. Immobilized molecular catalysts may be adapted to continuous flow processes. However, poor stability is a major drawback to immobilized metal complex catalysts. Significant efforts have been applied toward improving catalyst stability, not only through designing the catalytic functional component, but also through optimizing the linker structure [6–10].

We recently developed a new tripodal linker unit with three allylsilyl or isopropoxysilyl leaving groups (Scheme 1) [10]. This linker unit can be tightly bound to the surface of a silica support via three independent Si–O–Si bonds. In fact, organo-modified silica with a grafted tripodal linker unit (**A**) exhibited a higher hydrothermal stability to guard against leaching of organic moieties than silica modified with conventional trialkoxysilanes [10]. The tripodal linker unit additionally contains a bromopropyl moiety to which various organic functional molecules, including auxiliary ligands for metal complexes, may be attached. Therefore, this linker unit functions as a rigid scaffold to prevent grafted organic functional moieties from leaving the support.

Here, we report application of the tripodal linker unit to the immobilization of palladium amine complex catalysts on mesoporous silica supports, and we describe the use of the tethered catalysts in the Suzuki–Miyaura coupling reaction. The Suzuki–Miyaura reaction is a powerful and versatile tool for synthesizing organic compounds that can be utilized as organic electronic materials or intermediates for pharmaceuticals and agricultural chemicals [11]. Many publications have focused on the development of silica-supported palladium complexes or palladium nanoparticle catalysts for the Suzuki–Miyaura coupling reaction [12–43], but in view of the importance of the reaction, there is a continuing need to develop more efficient and recyclable catalysts.

Several reports have been published in recent years that show that the active species in the Suzuki–Miyaura coupling reaction via silica- or polymer-supported palladium catalysts are either (i)

* Corresponding authors at: Molecular Catalysis Group, Research Institute for Innovation in Sustainable Chemistry (ISC), National Institute of Advanced Industrial Science and Technology (AIST), Tsukuba Central 5, 1-1-1 Higashi, Tsukuba, Ibaraki 305-8565, Japan. Tel.: +81 29 861 9399; fax: +81 29 861 4559.
E-mail addresses: s-onozawa@aist.go.jp (S.-y. Onozawa), h.yasuda@aist.go.jp (H. Yasuda).

1381-1169/$ – see front matter © 2011 Elsevier B.V. All rights reserved.
doi:10.1016/j.molcata.2011.04.012

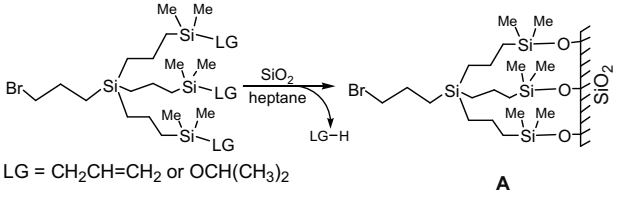

Scheme 1. Grafting of the tripodal linker unit onto the silica surface.

soluble palladium species leached into the reaction solution (homogeneous catalysis) [34–42] or (ii) tethered palladium complexes or palladium nanoparticle surfaces on supports (heterogeneous catalysis) [23–33]. A fraction of the palladium species (i) then re-deposit onto the ligands (or supports) after the reaction has gone to completion [43]. Therefore, we hypothesized that firmly immobilizing the ligands onto supports via a tripodal linker unit would bring about better recyclability in either catalysis.

2. Experimental

2.1. Materials

All chemicals were reagent grade and were used without further purification. A methylamine solution in tetrahydrofuran (THF) (2.0 mol/L) and a dimethylamine solution in THF (2.0 mol/L) were obtained from Sigma–Aldrich Co. *N*,*N*-Dimethylethylenediamine was purchased from Tokyo Chemical Industry Co., Ltd. 3-Bromopropyltriethoxysilane was purchased from Shin-Etsu Chemical Co., Ltd. Palladium(II) acetate was supplied by N.E. Chemcat Co. Ordered mesoporous silica with a 2D hexagonal structure (TMPS-4) [44], used as a silica support, was supplied by Taiyo Kagaku Co., Ltd. The specific surface area, pore volume, and average pore size were 1039 m^2/g, 1.46 cm^3/g, and 3.8 nm, respectively. Mesoporous silica was dried in vacuo at 80 °C for 3 h prior to use.

2.2. Preparation of amino-functionalized silica

The structures of the organic-functionalized silica materials used in this study are summarized in Fig. 1. 3-Bromopropyl-functionalized silica containing the tripodal linker unit (**A**) was prepared by grafting (3-bromopropyltris[3-(dimethylisopropoxysilyl)propyl]silane) onto mesoporous silica according to a procedure described previously [10]. The 3-bromopropyl-functionalized silica **A** was dried in vacuo at 80 °C for 3 h prior to use in further amination reactions. 3-Methylaminopropyl-functionalized silica (**B**), 3-dimethylaminopropyl-functionalized silica (**C**), and *N*,*N*-dimethylethylenediaminopropyl-functionalized silica (**D**) were prepared by reacting **A** with methylamine, dimethylamine, and *N*,*N*-dimethylethylenediamine, respectively. The reactions were carried out in Schlenk tubes (30 mL) under a nitrogen atmosphere. A typical procedure for the preparation of **B** was as follows: A mixture of **A** (1 g) and methylamine (20 mmol) in THF (10 mL) was stirred at 45 °C for 20 h. The resulting solid was filtered, washed with methanol, and dried in vacuo at 80 °C for 3 h. 3-Bromopropyl-functionalized silica containing the conventional linker (**E**) was prepared by reacting 3-bromopropyltriethoxysilane with mesoporous silica in heptane under reflux for 24 h under nitrogen. 3-Methylaminopropyl-functionalized silica (**F**) was prepared by reacting **E** with methylamine in a similar manner.

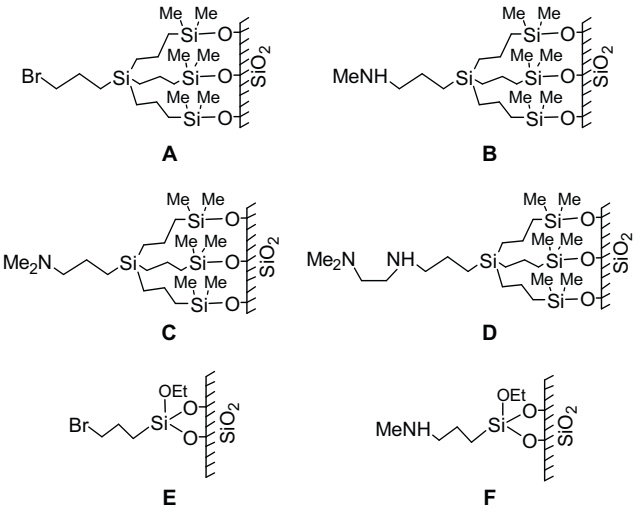

Fig. 1. Organic-functionalized silica materials.

2.3. Preparation of the palladium catalysts

Mesoporous silica-immobilized amino-palladium complex catalysts were prepared by reacting amino-functionalized silicas **B**–**D** and **F** with palladium acetate. **B**–**D** and **F** were dried in vacuo at 80 °C for 3 h prior to use in complexation reactions. A typical procedure for the preparation of a silica-immobilized methylamino-palladium complex with a ligand-to-palladium molar ratio of 1.3:1 was as follows: A mixture of **B** (1 g) and palladium acetate (83 mg) in THF (5 mL) was stirred at room temperature for 3 h under nitrogen. The resulting solid was filtered, washed with THF, and dried in vacuo at 80 °C for 3 h. The palladium concentration in the resulting filtrate was measured by ICP-OES to determine the extent of palladium loading on silica. All prepared catalysts were handled in air.

2.4. Characterization

Powder X-ray diffraction (XRD) data were acquired on a Bruker AXS D8-Advance X-ray diffractometer using Cu *K*α radiation. Nitrogen adsorption/desorption isotherms were measured at −196 °C using a Bel Japan BELSORP-mini II analyzer. Organic-functionalized silica samples were heated under vacuum at 80 °C for 3 h prior to the measurements. Specific surface areas were calculated using the BET method. The pore size distribution was obtained by the BJH method applied to the adsorption branch of the nitrogen adsorption/desorption isotherm. Scanning transmission electron microscopy (STEM) images were taken on a Hitachi HD-2000 microscope with an acceleration voltage of 200 kV. Solid-state ^{29}Si and ^{13}C cross-polarization/magic angle spinning (CP/MAS) NMR spectra were recorded on a Bruker AVANCE 400WB spectrometer operated at 79.5 or 100.6 MHz for ^{29}Si or ^{13}C, respectively, and using a 4 mm CP/MAS probe head. A typical spinning rate was 12.5 kHz, and CP contact times were 2.0 and 3.5 ms for ^{13}C and ^{29}Si CP/MAS, respectively. Pd *K*-edge extended X-ray absorption fine structure (EXAFS) measurements were carried out at the NW10A beamline at the Photon Factory Advanced Ring (PF-AR) in the Institute of Materials Structure Science, High Energy Accelerator Research Organization (IMSS-KEK). All spectra were measured using a Si(3 1 1) double-crystal monochromator in transmission mode at room temperature. The samples (40–70 mg) were placed in an EXAFS cell with an optical path length of 15 mm and polypropylene film windows. Analysis of EXAFS data was conducted using the commercially available analytical program REX2000 (Rigaku Co.). Elemental analysis of carbon and nitrogen compositions was conducted using a CE Instruments EA 1112 elemental analyzer. Elemental analysis of bromine was conducted using a Dionex ICS-2000 ion chromatograph. Palladium concentrations in solutions were determined using a Thermo Fisher Scientific

iCAP 6500 Duo inductively coupled plasma-optical emission spectrometer (ICP-OES) and an Agilent 7500ce ICP-mass spectrometer (ICP-MS).

2.5. Catalytic testing

The Suzuki–Miyaura coupling reaction of aryl bromide and phenylboronic acid was carried out in a Schlenk tube (30 mL) under a nitrogen atmosphere. A typical experimental procedure was as follows: A mixture of aryl bromide (3.0 mmol), phenylboronic acid (3.3 mmol), potassium carbonate (6.0 mmol), the catalyst (0.05 mol% with respect to palladium), and 4-*tert*-butyltoluene (430 mg) as an internal standard for gas chromatograph (GC) analysis were stirred in toluene (3 mL) at 100 °C. The reaction mixture was periodically sampled to follow the progress of the reaction by GC. After the reaction, the catalyst was separated by centrifugation, and the supernatant was analyzed on a Shimadzu GC-14B GC equipped with a thermal conductivity detector and a column (2 mm × 3 m) packed with 3% OV-101 on Chromosorb WHP (100/120 mesh) to determine the product yields. To quantify the extent of palladium leaching, the palladium concentration in the supernatant was measured by ICP-MS after the catalyst was thoroughly removed by filtration using a 0.2 μm PTFE membrane filter.

2.6. Hot filtration

The Suzuki–Miyaura coupling reaction of 4-bromobenzoic acid ethyl ester (3.0 mmol) and phenylboronic acid (3.3 mmol) was conducted at 100 °C for 3 min in the presence of potassium carbonate (6.0 mmol), the catalyst (0.05 mol% with respect to palladium), and 4-*tert*-butyltoluene (internal standard, 430 mg) in toluene (3 mL). Then, the reaction mixture was filtered under hot conditions using a 0.2 μm PTFE membrane filter. The product yield and the palladium concentration in the filtrate were determined by GC and ICP-MS, respectively. Subsequently, phenyl boronic acid (3.3 mmol) and potassium carbonate (6.0 mmol) were added to the filtrate, and the mixture was stirred at 100 °C for 3 h.

2.7. Catalyst recycling

The Suzuki–Miyaura coupling reaction between 4-bromobenzoic acid ethyl ester (3.0 mmol) and phenylboronic acid (3.3 mmol) was conducted at 100 °C for 2 h in the presence of potassium carbonate (6.0 mmol), the catalyst (0.05 or 0.25 mol% with respect to palladium), and 4-*tert*-butyltoluene (internal standard, 430 mg) in toluene (3 mL). The resulting suspension was centrifuged, and the supernatant was removed by decantation. The reaction tube was subsequently recharged with 4-bromobenzoic acid ethyl ester, phenylboronic acid, potassium carbonate, 4-*tert*-butyltoluene (internal standard), and toluene, and the reaction was repeated.

3. Results and discussion

3.1. Preparation and characterization of the amino-functionalized silica

The 3-bromopropyl-functionalized silica material **A**, onto which the tripodal linker unit was grafted, was prepared from 3-bromopropyltris[3-(dimethylisopropoxysilyl)propyl]silane and mesoporous silica (TMPS-4), as described previously [10]. The effect of the linker structure on the catalytic performance was evaluated by comparison with 3-bromopropyl silica **E** that had been functionalized using conventional triethoxysilane. The organic contents in **A** and **E** were determined by carbon elemental analysis to be 0.42 and 0.76 mmol/g, respectively. Subsequent treatment of **A** and **E** with methylamine in THF converted the bromo groups in **A** and **E** into methylamino groups to yield the amino-functionalized silica materials **B** and **F**, respectively. Amination of **A** with dimethylamine and *N*,*N*-dimethylethylenediamine gave the amino-functionalized silica materials **C** and **D**, respectively [45]. The bromine content of each amino-functionalized silica sample **B**–**D** and **F** was less than 0.1 wt% according to bromine analysis, indicating quantitative conversion of the bromo groups in **A** and **E** into amino groups on the silica surfaces. Table 1 lists the organic content of each of the materials **A**–**F**. The organic content in **B**–**D** and **F** was quantified by nitrogen elemental analysis. As **A** was aminated to give **B**–**D**, the organic content decreased slightly from 0.42 to 0.40–0.31 mmol/g, whereas amination of **E** to give **F** significantly reduced the organic content from 0.76 to 0.48 mmol/g [46]. This showed that the tripodal anchoring was highly effective at minimizing leaching of organic groups from the silica surface during functional group transformation.

Table 1
Compositional and textural data for the organic-functionalized silica materials **A**–**F**.

Material	Loading (mmol/g)	Surface area (m^2/g)	Pore volume (cm^3/g)	Pore size (nm)
TMPS-4	–	1039	1.46	3.8
A	0.42[a]	861	1.07	3.3
B	0.37[b]	869	1.05	3.3
C	0.40[b]	804	1.04	3.3
D	0.31[b]	791	1.01	3.3
E	0.76[a]	890	1.06	3.3
F	0.48[b]	890	1.18	3.7

[a] Determined by elemental analysis of carbon.
[b] Determined by elemental analysis of nitrogen.

The high stability of the grafted tripodal linkers under amination conditions was further corroborated by ^{29}Si CP/MAS spectroscopy. Fig. 2(a) shows the ^{29}Si CP/MAS spectra of **A** and **B**. Both samples displayed broad peaks around δ −100 ppm due to Q^3 and Q^4 silicon in silica as well as two peaks corresponding to a single tetraalkyl-coordinated silicon center (δ 2 ppm) and three trialkylmonooxygen-coordinated silicon centers (δ 14 ppm) [47]. It should be noted that the two ^{29}Si CP/MAS peaks in the organosilane regions of the spectra of samples **A** and **B** were nearly identical. Fig. 2(b) displays the ^{29}Si CP/MAS spectra of **E** and **F**. The spectrum of **E** exhibited a major peak assigned to T^2 silicon (δ −57 ppm) and a minor peak assigned to T^1 silicon (δ −48 ppm). The peak due to T^3 silicon was very small, indicating that the bromopropyl group in **E** was bound to silica via one or two Si–O–Si bonds. In the spectrum of **F**, the T^1 peak disappeared, the T^2 peak decreased, and the T^3 peak (δ −66 ppm) increased. These observations suggested that detachment of the organic moieties and redistribution of the T^1, T^2, and T^3 species in **E** occurred via cleavage and reformation of the Si–O–Si linkage during amination. These results clearly demonstrated that three independent Si–O–Si bonds formed with the tripodal linker unit prevented the grafted organic groups from leaving the silica support during the amination process.

The successful transformation of the bromo group in **A** into a methylamino group was confirmed by ^{13}C CP/MAS spectroscopy. Fig. 3 shows the ^{13}C CP/MAS spectra of **A** and **B**. The carbon "a" in **B** exhibited approximately the same chemical shift as **A**, whereas conversion of the bromo group into a methylamino group shifted the peak corresponding to the β-carbon ("b") of the bromopropyl group in **A** (δ 27 ppm) upfield to around δ 21 ppm (overlapping with the carbon "e") in **B**. The carbon "c" was also shifted slightly upfield after amination.

The XRD patterns of the organic-functionalized silica materials **A**–**F** were similar to that of parent mesoporous silica [44], exhibiting a strong (1 0 0) reflection peak and weak (1 1 0) and (2 0 0) peaks characteristic of hexagonally ordered mesoporous materials. Thus,

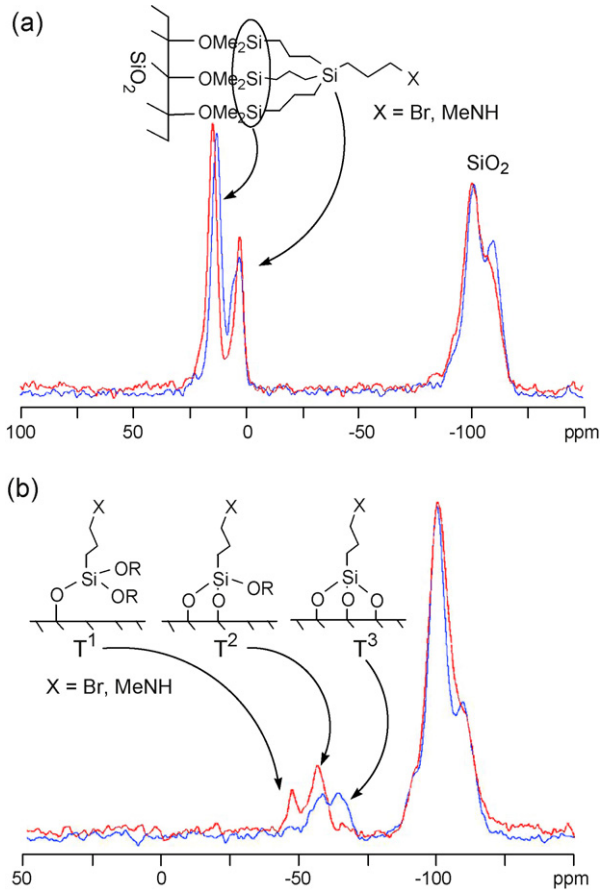

Fig. 2. ^{29}Si CP/MAS spectra of (a) organic-functionalized silicas **A** (red line) and **B** (blue line), and (b) organic-functionalized silicas **E** (red line) and **F** (blue line). (For interpretation of the references to color in this figure legend, the reader is referred to the web version of the article.)

grafting the tripodal linker unit or 3-bromopropyltriethoxysilane and subsequent introduction of the amino groups preserved the mesoporous structure. The nitrogen adsorption/desorption isotherms of **A**–**F** showed type IV sorption curves that are typical of mesoporous structures. Table 1 displays the textural data. Grafting of the bulky tripodal linkers reduced the pore volume from 1.46 to 1.07 cm^3/g and narrowed the average pore size from 3.8 to

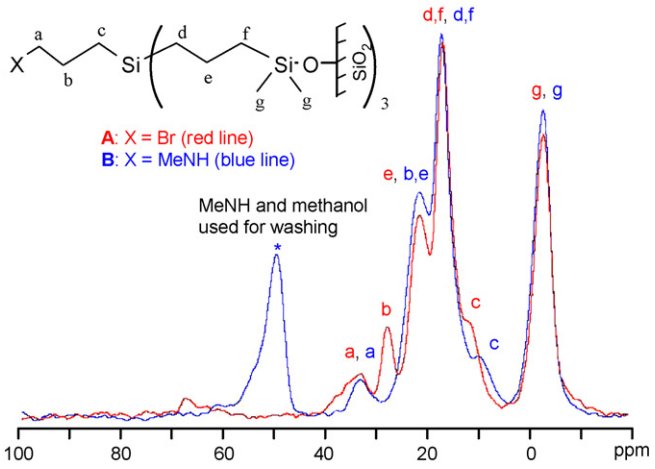

Fig. 3. ^{13}C CP/MAS spectra of organic-functionalized silicas **A** (red line) and **B** (blue line). (For interpretation of the references to color in this figure legend, the reader is referred to the web version of the article.)

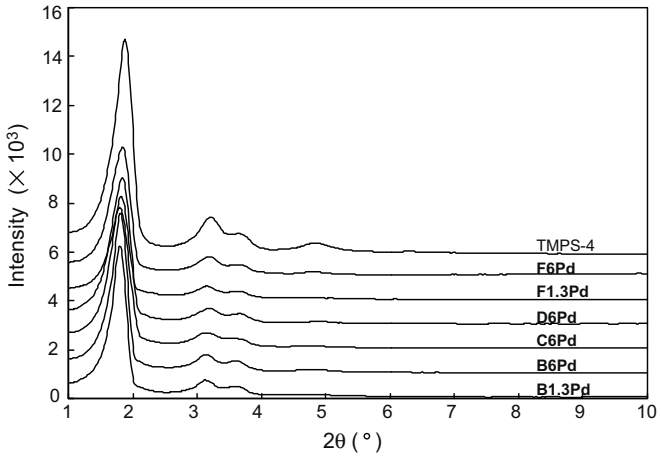

Fig. 4. XRD patterns of the catalysts **BnPd**–**FnPd** and the mesoporous silica support (TMPS-4).

3.3 nm, whereas subsequent amination minimally affected the pore volume and pore size. 3-Bromopropyl and 3-aminopropyl functionalizations decreased the specific surface areas, however, **B**–**D** and **F** maintained high surface areas (>790 m^2/g).

3.2. Preparation and characterization of the palladium catalysts

The immobilized amino-palladium complex catalysts were prepared by reacting amino-functionalized silicas **B**–**D** and **F** with palladium acetate in THF at room temperature. After the reaction, the solid was filtered, washed with THF, and dried in vacuo at 80 °C. To investigate the influence of the molar ratio between the amino ligand and palladium on the catalytic performance, catalysts **B** and **F** with different palladium loadings (ligand-to-Pd molar ratios of 1:1, 3:1, or 6:1) were prepared by varying the concentration of $Pd(OAc)_2$ in the THF solution. Hereafter, the palladium catalysts will be represented by **MnPd**, where *M* and *n* are the type of amino-functionalized silica and the molar ratio between the amino ligand and palladium, respectively. The palladium concentration in the filtrate of the catalyst preparation was measured by ICP-OES. The filtrates obtained from the preparation of **B1.3Pd** and **F1.3Pd** contained 21.9% and 24.8% unreacted $Pd(OAc)_2$, respectively. Consequently, the actual ligand-to-Pd molar ratios in the **B1.3Pd** and **F1.3Pd** catalysts were 1.28:1 and 1.33:1, respectively. The other prepared catalysts yielded palladium concentrations in the filtrates that were less than the quantification limit of ICP-OES analysis. Thus, **B3Pd**, **B6Pd**, **C6Pd**, **D6Pd**, **F3Pd**, and **F6Pd** contained virtually all of the added palladium.

Fig. 4 shows the XRD patterns for the prepared catalysts **BnPd**–**FnPd** and the mesoporous silica support (TMPS-4). All samples exhibited three clear peaks in the 2θ range of 1–4° that were characteristic of hexagonally ordered mesophases, indicating that the regular structure of the mesoporous silica remained unchanged after palladium loading. Diffraction peaks due to palladium metal were not detected in the fresh **BnPd**–**FnPd** samples over the 2θ region of 40–50°. The mesoporosity of each catalyst **BnPd**–**FnPd** was measured by nitrogen adsorption/desorption measurements (Fig. 5). All catalysts exhibited type IV isotherms, confirming that the mesoporous structure was retained after palladium loading. The mesopores, therefore, were not plugged by formation of palladium nanoparticles. Table 2 summarizes the compositional and textural data of the catalysts. The pore volume and pore size were nearly unchanged before and after palladium loading. The changes in the specific surface areas were also small.

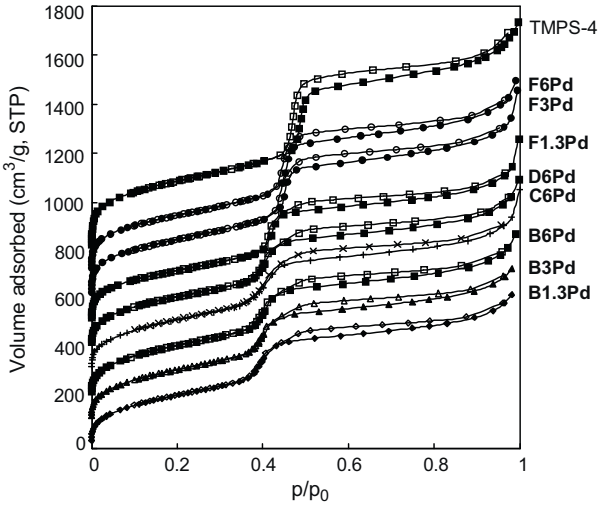

Fig. 5. Nitrogen adsorption/desorption isotherms of the catalysts **BnPd**–**FnPd** and the mesoporous silica support (TMPS-4). The isotherms are offset vertically, from **B3Pd** to TMPS-4.

Table 2
Compositional and textural data for the catalysts **BnPd**–**FnPd**.

Catalyst	Pd content[a] (wt%)	Ligand:Pd molar ratio	Surface area (m^2/g)	Pore volume (cm^3/g)	Pore size (nm)
B1.3Pd	3.48	1.28:1	803	1.07	3.3
B3Pd	1.48	3:1	811	1.07	3.3
B6Pd	0.74	6:1	808	1.04	3.3
C6Pd	0.70	6:1	828	1.07	3.3
D6Pd	0.55	6:1	799	1.03	3.3
F1.3Pd	3.79	1.33:1	804	1.09	3.3
F3Pd	1.68	3:1	899	1.27	3.7
F6Pd	0.82	6:1	895	1.23	3.7

[a] Determined from the difference between the Pd content in the filtrates of the catalyst preparations, measured by ICP-OES, and the initial Pd content.

To explore the local structure of palladium on amino-functionalized silica, Pd *K*-edge EXAFS measurements were performed. Fig. 6 shows the Fourier transforms (FT) of the k^3-weighted EXAFS spectra for the catalysts **BnPd** and the reference materials, including tetraamminepalladium(II) chloride, $Pd(OAc)_2$, and Pd foil. Because the phase shift was uncorrected, the radial distance (r) from a palladium atom, shown in Fig. 6, was shifted from the actual bond distance. A peak around 2.5 Å in the spectrum of the Pd foil, assigned to scattering from the nearest neighbor palladium atoms in a metallic palladium cluster, was not observed in the spectra of **B1.3Pd**, **B3Pd**, and **B6Pd**. The FT profiles of these samples were similar to those of $[Pd(NH_3)_4]Cl_2$ and $Pd(OAc)_2$ consisting of an isolated palladium atom with a square planar PdE_4 (E = N or O) structure locating Pd–E at the distance of 2.02 or 2.03 Å, respectively [48,49]. Because the parameters associated with the phase shift function and backscattering amplitude of Pd–N are similar to those of Pd–O, curve-fitting analysis of the EXAFS spectra cannot distinguish between nitrogen and oxygen coordinated to palladium. Curve-fitting analysis of the first shell in the FT of EXAFS for the catalysts **BnPd**–**D6Pd** was carried out using parameters for Pd–N scattering extracted from $[Pd(NH_3)_4]Cl_2$ (Table 3). The optimum fitting results for **BnPd**–**D6Pd** were 3.5–3.7 for the coordination numbers (CN) and around 2.02 Å for the distance (r). These results indicated that palladium was most likely surrounded by four nitrogen and/or oxygen atoms, in other words, the palladium was loaded onto the amino-functionalized silica surfaces **B**–**D** as palladium complexes, without aggregating to form palladium particles.

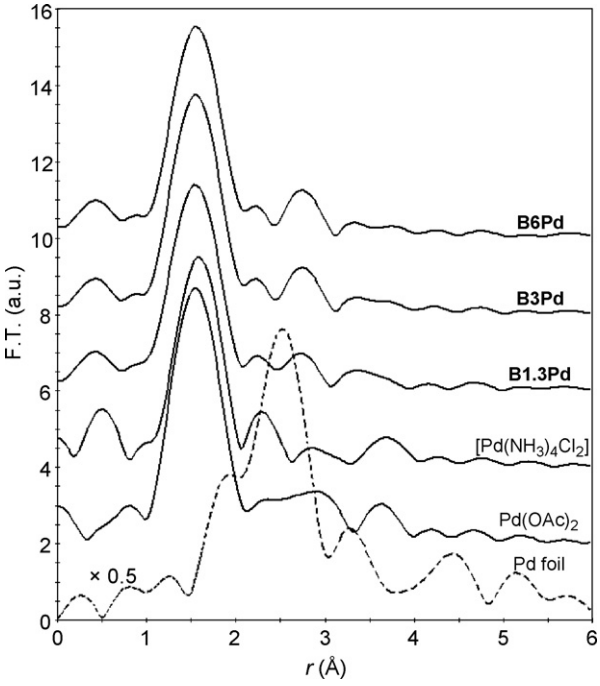

Fig. 6. Fourier transforms of the k^3-weighted Pd *K*-edge EXAFS spectra for the catalysts **BnPd** and $[Pd(NH_3)_4]Cl_2$, $Pd(OAc)_2$, and Pd foil (dashed line), as reference materials.

Table 3
Curve-fitting results of Pd *K*-edge EXAFS spectra for the catalysts **BnPd**–**DnPd**[a].

Catalyst	CN[b]	r (Å)[c]	ΔE (eV)[d]	R factor (%)[e]
B1.3Pd	3.5 ± 0.5	2.01 ± 0.01	−6.8 ± 2.8	0.4
B3Pd	3.7 ± 0.5	2.02 ± 0.02	−5.8 ± 3.0	0.5
B6Pd	3.6 ± 0.6	2.03 ± 0.02	−5.4 ± 3.0	0.6
C6Pd	3.7 ± 0.9	2.02 ± 0.02	−6.5 ± 3.0	1.7
D6Pd	3.7 ± 0.5	2.01 ± 0.02	−0.4 ± 3.5	0.9

[a] The Debye–Waller factor was fixed at 0.03 Å for all analyses.
[b] Coordination number of Pd-E (E = N or O).
[c] Radial distance of E from Pd.
[d] Difference in the edge energy between a reference compound and the catalyst.
[e] $R = \sum (k^3\chi_{obs} - k^3\chi_{cal})^2 / \sum (k^3\chi_{obs})^2 \times 100$.

3.3. Catalysis for the Suzuki–Miyaura coupling reaction

The catalytic performance of each prepared silica-immobilized amino-palladium complex was probed in the Suzuki–Miyaura coupling reaction between aryl bromides and phenylboronic acid to give the corresponding biaryls (Scheme 2). Initially, the influence of the type of the amino group on the catalytic activity was investigated using the catalysts **B6Pd**, **C6Pd**, and **D6Pd** for the reaction between 4-bromobenzoic acid ethyl ester and phenylboronic acid (Table 4). The reaction was conducted in toluene at 100 °C for 3 h, using potassium carbonate as a base. The quantity of catalyst was adjusted to 0.05 mol% with respect to the palladium. **B6Pd**, which included a secondary amine ligand, gave a higher yield than **C6Pd**, which included a tertiary amine (entries 1 and 2). The chelating ligand-containing catalyst **D6Pd** showed low catalytic activity. Thus, we focused on the **BnPd** series for further studies.

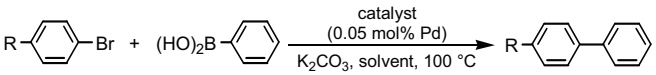

Scheme 2. The Suzuki–Miyaura coupling reaction.

Table 4
Results of the Suzuki–Miyaura coupling reaction between aryl bromides and phenylboronic acid using the catalysts **BnPd**–**DnPd**[a].

Entry	Catalyst	R	Time (h)	Yield (%)[b]
1	**B6Pd**	COOEt	3	98
2	**C6Pd**	COOEt	3	93
3	**D6Pd**	COOEt	3	21
4	**B6Pd**	COOEt	0.5	94
5	**B6Pd**	Me	0.5	93
6	**B6Pd**	OMe	0.5	95
7	**B6Pd**	CN	0.5	100

[a] Reaction conditions: aryl bromides (3.0 mmol), phenylboronic acid (3.3 mmol), K_2CO_3 (6.0 mmol), catalyst (0.05 mol% Pd), toluene (3 mL), 100 °C.
[b] Determined by GC analysis using 4-*tert*-butyltoluene as an internal standard.

Table 5
Results of the Suzuki–Miyaura coupling reaction between 4-bromobenzoic acid ethyl ester and phenylboronic acid using the catalysts **BnPd** and **FnPd**[a].

Entry	Catalyst	Yield (%)[b]	Pd leaching (%)[c]
1	**B1.3Pd**	97	0.13
2	**B3Pd**	94	0.13
3	**B6Pd**	98	0.098
4	**F1.3Pd**	89	0.81
5	**F3Pd**	97	0.22
6	**F6Pd**	98	0.29

[a] Reaction conditions: 4-bromobenzoic acid ethyl ester (3.0 mmol), phenylboronic acid (3.3 mmol), K_2CO_3 (6.0 mmol), catalyst (0.05 mol% on Pd), toluene (3 mL), 100 °C, 2 h.
[b] Determined by GC analysis using 4-*tert*-butyltoluene as an internal standard.
[c] Determined by ICP-MS as a percentage of the initial Pd content.

B6Pd gave the product in good yield, even if the reaction times were shortened from 3 h to 0.5 h. Additionally, good yields were obtained even if the less reactive electron-rich aryl bromides were used, such as 4-bromoanisole or 4-bromotoluene (entries 5 and 6). Fig. 7 shows the time courses of the **B6Pd**-catalyzed Suzuki–Miyaura coupling of 4-bromobenzoic acid ethyl ester and phenylboronic acid in various solvents. A nonpolar solvent, toluene, gave the best results, whereas the polar solvents, such as dimethylformamide (DMF), 1,4-dioxane, or cyclopentyl methyl ether (CPME), decreased the reaction rate.

Suzuki–Miyaura coupling reactions in the presence of supported palladium catalysts proceed via both homogeneous and heterogeneous mechanisms [23–43], as mentioned in Section 1. The active species of the Suzuki–Miyaura reaction catalyzed by **B6Pd** was investigated by performing hot filtration experiments. Immediately after the reaction between 4-bromobenzoic acid ethyl ester and phenylboronic acid in toluene at 100 °C for 3 min, the solid components, including the catalyst, were removed by filtration under hot conditions. The yield of the corresponding biaryl in the filtrate was 14%, which was determined by GC analysis. Subsequently, fresh reagents (phenylboronic acid and potassium carbonate) were added to the filtrate, and the mixture was stirred at 100 °C for 3 h in the absence of the solid-phase catalyst. The coupling reaction then proceeded to yield the product in 79%, strongly suggesting a substantial contribution to the present Suzuki–Miyaura coupling reaction from homogeneous catalysis due to dissolved palladium species from **B6Pd**. ICP-MS analysis of the filtrate obtained by hot filtration disclosed that 5% palladium atoms in **B6Pd** were eluted. In contrast, the palladium leaching level in the filtrate obtained by filtration at room temperature after 2 h of the reaction was only 0.098% (*vide infra*), indicating that dissolved palladium species effectively re-deposited back onto the amino-functionalized silica support during cooling of the reaction mixture to room temperature, after completion of the reaction. Palladium can re-deposit once aryl halide is consumed in the Suzuki–Miyaura coupling [34]. On the basis of these observations, the order of activity among catalysts with different amino ligands (**B6Pd** > **C6Pd** » **D6Pd**) (Table 4) seems to reflect the degree of palladium dissociation from the palladium complexes immobilized on the silica support.

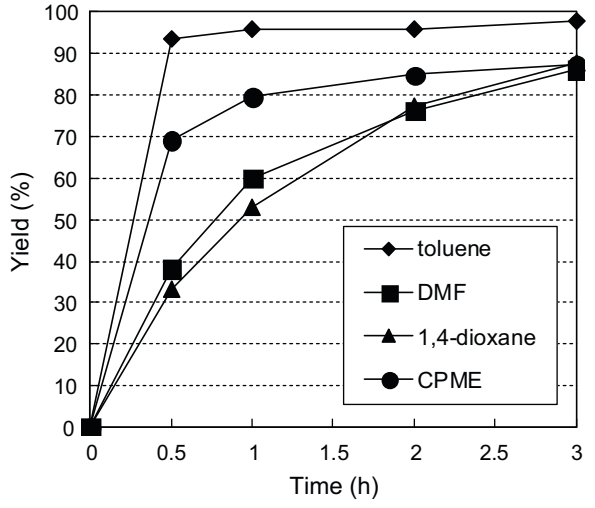

Fig. 7. Time courses of the **B6Pd**-catalyzed Suzuki–Miyaura coupling reaction between 4-bromobenzoic acid ethyl ester and phenylboronic acid in various solvents.

Next, the influence of the linker structure on the catalytic activity, palladium leaching, and catalyst recyclability was assessed using the **BnPd** and **FnPd** series. All fresh catalyst samples gave good yields in 2 h for the Suzuki–Miyaura coupling of 4-bromobenzoic acid ethyl ester and phenylboronic acid (Table 5). After the reaction, the reaction mixture was cooled to room temperature, then the catalyst was separated by filtration, and the extent of palladium leaching into the reaction solution was determined by ICP-MS. All catalysts showed relatively low levels of palladium leaching (below 1% of the initial Pd content). It should be noted that at each ligand-to-Pd ratio, the leaching level of **BnPd** (0.098–0.13%) was lower than that of **FnPd** (0.22–0.81%). Although the tripodal linker of **BnPd** could not inhibit decoordination of palladium from the methylamino ligand, firm immobilization of the amino ligand via the tripodal linker most likely effectively prevented the amino-palladium complex from leaving the silica support (cleavage of the Si–O–Si linkage) during the Suzuki–Miyaura coupling reaction. In addition, a sufficiency of the amino ligand available to recapture dissolved palladium species after completing the reaction would remain on the silica support due to the tripodal anchoring (*vide infra*).

The catalyst recyclability of **BnPd** and **FnPd** was assessed by performing the reaction between 4-bromobenzoic acid ethyl ester and phenylboronic acid, removing the reaction supernatant via centrifugation and decantation, and recharging the reaction tube with the substrates, a base, and a solvent, to allow the reaction to proceed again. The catalyst recycling experiments were initially conducted using only small amounts of catalyst (0.05 mol% palladium) to emphasize any effects of catalyst deterioration throughout the reaction–recycling process. Fig. 8 shows the time courses of the repeated reactions. Although the catalytic activities were similar among the fresh catalysts, as shown in Table 5, obvious differences in the reaction rate were observed in the second and third runs. The recyclability of **BnPd** and **FnPd** critically depended on the ligand-to-Pd ratio. The catalyst that contained a larger ligand-to-Pd ratio showed better recyclability. This observation might be explained by the different degree of stabilization of amino-palladium complexes which are precursors of soluble palladium species by the presence of excess amino ligand. The linker structure also considerably affected the catalyst recyclability. At each ligand-to-Pd ratio, replacing the conventional trialkoxy-type linker (**FnPd**) with

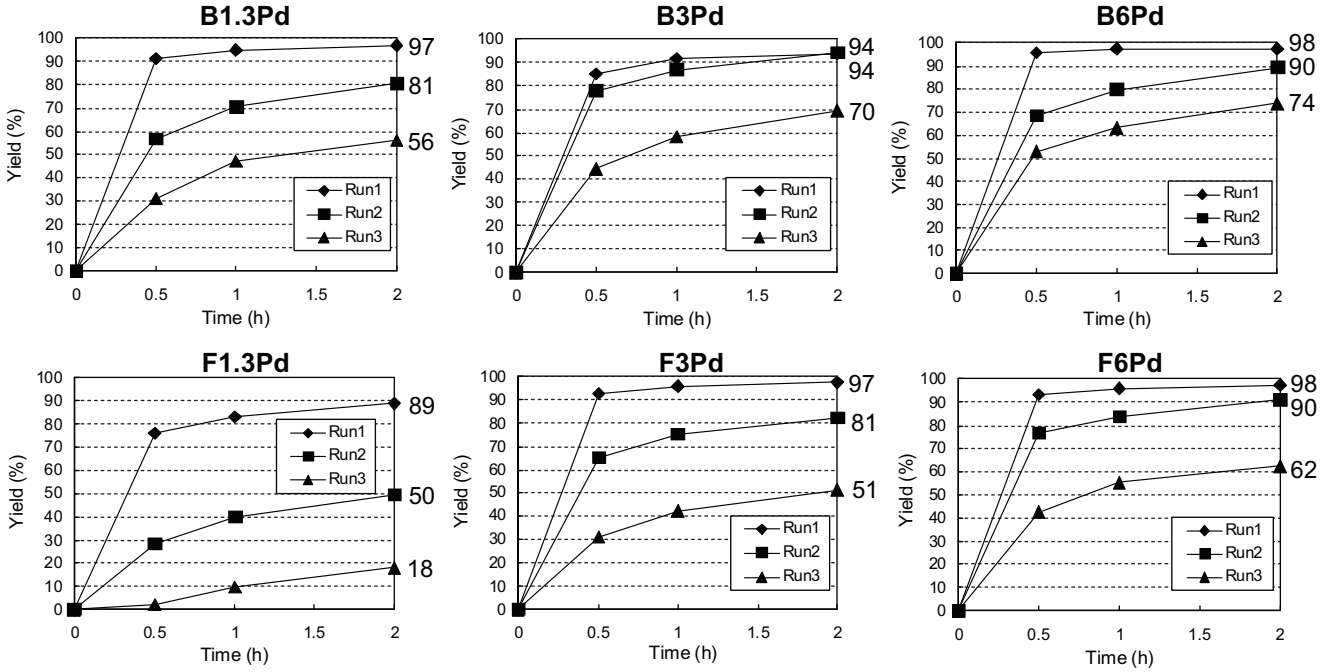

Fig. 8. Time courses for the repeated Suzuki–Miyaura coupling reactions between 4-bromobenzoic acid ethyl ester and phenylboronic acid using the catalysts **BnPd** and **FnPd**. The yields after 2 h are presented in the right side of the plots.

the tripodal-type linker (**BnPd**) improved the recyclability. The most significant difference in recyclability was observed between **B1.3Pd** and **F1.3Pd**, with an unfavorable ligand-to-Pd ratio. This difference could not be explained by the difference in the loss of palladium due to leaching because the second runs of **B1.3Pd** and **F1.3Pd** were expected to contain 0.0499 and 0.0496 mol% palladium, respectively, judging from the palladium leaching measurements (Table 5).

Fig. 9 displays the STEM images of fresh **B1.3Pd** and **F1.3Pd** as well as recovered **B1.3Pd** and **F1.3Pd** after the first catalytic run. Aggregated palladium metal particles were not observed in either STEM image of the fresh **B1.3Pd** or **F1.3Pd**, consistent with the results of XRD and EXAFS analysis. In contrast, palladium nanoparticles were found in used **B1.3Pd** and **F1.3Pd** (Fig. 9(c) and (d)). The average size of the palladium particles in used **F1.3Pd** (*ca.* 4–10 nm) was clearly larger than that in used **B1.3Pd** (*ca.* 1–2 nm). These

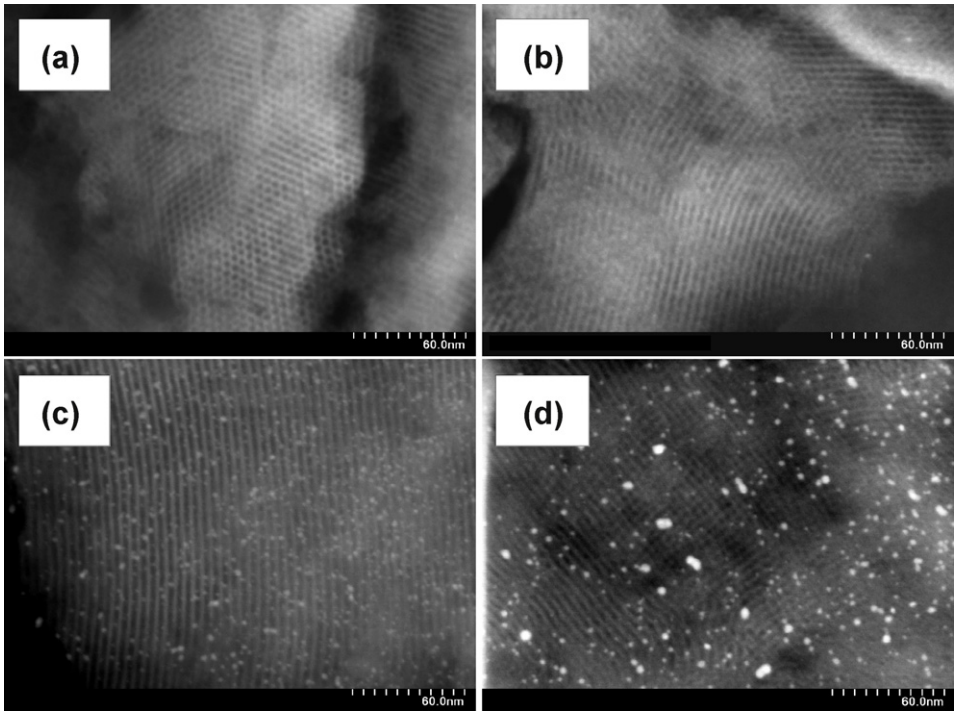

Fig. 9. STEM images of (a) fresh catalyst **B1.3Pd**, (b) fresh **F1.3Pd**, (c) used **B1.3Pd** after the first catalytic run in Fig. 8, and (d) used **F1.3Pd** after the first catalytic run in Fig. 8.

Table 6
Catalyst recycling experiments for the **B6Pd**-catalyzed Suzuki–Miyaura coupling reaction between 4-bromobenzoic acid ethyl ester and phenylboronic acid[a].

Catalytic run	Time (h)	Yield (%)[b]
1st	2	93
2nd	2	97
3rd	2	93
4th	2	>99
5th	2	73
5th	6	93

[a] Reaction conditions: 4-bromobenzoic acid ethyl ester (3.0 mmol), phenylboronic acid (3.3 mmol), K_2CO_3 (6.0 mmol), **B6Pd** (0.25 mol% Pd), toluene (3 mL), 100 °C. Procedures for catalyst recycling, *see* text.
[b] Determined by GC analysis using 4-*tert*-butyltoluene as an internal standard.

results suggest that deactivation is attributable to the deposition of the palladium species on the silica surface and their aggregation to form clusters and inactive large particles [50]. It is presumed that the better recyclability of **B1.3Pd** is associated with the harder formation of palladium metal particles on the silica surface during the reaction. Firm immobilization of the amino ligand via the tripodal linker should maintain the number of ligands available to stabilize the palladium complexes which are precursors of soluble active palladium species, and thus prevented the formation of palladium metal particles on the silica surface during the re-deposition process. Another possibility is that highly dispersed amino-palladium complexes smoothly produced active palladium species giving high catalytic activities for the Suzuki–Miyaura coupling. Because the bulky scaffold of the tripodal linker should inhibit agglomerated grafting of organic functional groups on a silica surface, the tripodal linker in **BnPd** is expected to effectively isolate the attached amino groups, thereby keeping the metal centers separate. Consequently, the tripodal linker unit maintained the amino-palladium complexes in a highly dispersed state, leading to improved recyclability of **BnPd**.

Finally, the catalyst recycling experiment was performed using **B6Pd** with an increased quantity of catalyst (0.25 mol% palladium). The results are presented in Table 6. The catalyst **B6Pd** could be reused through a fourth catalytic run without significant loss in yield, demonstrating the relatively high stability of **B6Pd**. Although the reaction rate decreased in the fifth run, the yield reached 93% after prolonged reaction time (6 h). Fig. 10 displays the ^{29}Si CP/MAS spectra of recovered **B6Pd** after the fifth catalytic run as well as fresh **B6Pd**. No significant changes in the ^{29}Si CP/MAS peaks in the organosilane region of **B6Pd** were observed before and after the catalytic runs. This result clearly demonstrated that grafting of the tripodal linker via three isolated Si–O–Si bonds was highly stable even under the reaction conditions.

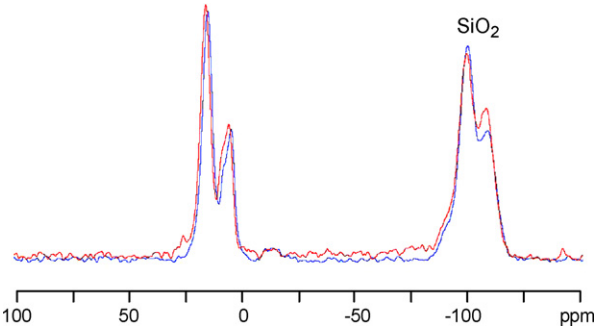

Fig. 10. ^{29}Si CP/MAS spectra of fresh catalyst **B6Pd** (red line) and recovered **B6Pd** after the fifth catalytic run in Table 6 (blue line). (For interpretation of the references to color in this figure legend, the reader is referred to the web version of the article.)

4. Conclusions

We successfully applied our tripodal linker unit to the preparation of mesoporous silica-immobilized amino-palladium complex catalysts for the Suzuki–Miyaura coupling reaction. Compared to conventional trialkoxy-type linkers, the tripodal linker is more advantageous and attractive in the following respects: (i) Tripodal anchoring prevented grafted organic groups from leaving the silica support during functional group transformations; (ii) Tripodal anchoring reduced the extent of metal leaching into the reaction solution after the catalytic reaction; (iii) Tripodal anchoring improved catalyst recyclability. 3-Bromopropyl-functionalized silica **A** is a versatile precursor for synthesizing other novel immobilized molecular catalysts because its bromo group can be easily converted into a variety of ligands, including phosphines and sulfides. Such efforts are currently underway in our group.

Acknowledgments

This research was financially supported by the Development of Microspace and Nanospace Reaction Environment Technology for Functional Materials Project of NEDO, Japan. The EXAFS experiments were performed under the approval of the Photon Factory Program Advisory Committee (Proposal No. 2009G048). We thank Ms. Michiyo Yoshinaga for assistance with catalytic experiments and Dr. Toshikazu Takahashi for helpful discussion on CP/MAS spectroscopy.

References

[1] A.P. Wight, M.E. Davis, Chem. Rev. 102 (2002) 3589.
[2] J.Y. Ying, C.P. Mehnert, M.S. Wong, Angew. Chem. Int. Ed. 38 (1999) 56.
[3] D. Brunel, A.C. Blanc, A. Galarneau, F. Fajula, Catal. Today 73 (2002) 139.
[4] A. Corma, H. Garcia, Adv. Synth. Catal. 348 (2006) 1391.
[5] N. End, K.-U. Schöning, Top. Curr. Chem. 242 (2004) 241.
[6] C. Merckle, S. Haubrich, J. Blümel, J. Organomet. Chem. 627 (2001) 44.
[7] T. Takahashi, T. Watahiki, S. Kitazume, H. Yasuda, T. Sakakura, Chem. Commun. (2006) 1664.
[8] N. Maity, S. Basu, M. Mapa, P.R. Rajamohanan, S. Ganapathy, C.S. Gopinath, S. Bhaduri, G.K. Lahiri, J. Catal. 242 (2006) 332.
[9] B. Pugin, H.-U. Blaser, Adv. Synth. Catal. 348 (2006) 1743.
[10] N. Fukaya, S. Onozawa, M. Ueda, K. Saitou, Y. Takagi, T. Sakakura, H. Yasuda, Chem. Lett. 39 (2010) 402.
[11] N. Miyaura, A. Suzuki, Chem. Rev. 95 (1995) 2457.
[12] J. Horniakova, T. Raja, Y. Kubota, Y. Sugi, J. Mol. Catal. A: Chem. 217 (2004) 73.
[13] B. Blanco, A. Mehdi, M. Moreno-Mañs, R. Pleixats, C. Reyè, Tetrahedron Lett. 45 (2004) 8789.
[14] R.B. Bedford, U.G. Singh, R.I. Walton, R.T. Williams, S.A. Davis, Chem. Mater. 17 (2005) 701.
[15] Q. Yang, S. Ma, J. Li, F. Xiao, H. Xiong, Chem. Commun. (2006) 2495.
[16] J.D. Webb, S. MacQuarrie, K. McEleney, C.M. Crudden, J. Catal. 252 (2007) 97.
[17] S. Tandukar, A. Sen, J. Mol. Catal. A: Chem. 268 (2007) 112.
[18] G. Budroni, A. Corma, H. García, A. Primo, J. Catal. 251 (2007) 345.
[19] R. Sayah, K. Glegoła, E. Framery, V. Dufaud, Adv. Synth. Catal. 349 (2007) 373.
[20] M. Trilla, R. Pleixats, M.W.C. Man, C. Bied, J.J.E. Moreau, Adv. Synth. Catal. 350 (2008) 577.
[21] M. Trilla, G. Borja, R. Pleixats, M.W.C. Man, C. Bied, J.J.E. Moreau, Adv. Synth. Catal. 350 (2008) 2566.
[22] K. Dhara, K. Sarkar, D. Srimani, S.K. Saha, P. Chattopadhyay, A. Bhaumik, Dalton Trans. 39 (2010) 6395.
[23] E.B. Mubofu, J.H. Clark, D.J. Macquarrie, Green Chem. 3 (2001) 23.
[24] Y.M.A. Yamada, K. Takeda, H. Takahashi, S. Ikegami, J. Org. Chem. 68 (2003) 7733.
[25] K. Shimizu, S. Koizumi, T. Hatamachi, H. Yoshida, S. Komai, T. Kodama, Y. Kitayama, J. Catal. 228 (2004) 141.
[26] S. Paul, J.H. Clark, Green Chem. 5 (2003) 635.
[27] C.M. Crudden, M. Sateesh, R. Lewis, J. Am. Chem. Soc. 127 (2005) 10045.
[28] M. Al-Hashimi, A. Qazi, A.C. Sullivan, J.R.H. Wilson, J. Mol. Catal. A: Chem. 278 (2007) 160.
[29] M. Cai, J. Sha, Q. Xu, J. Mol. Catal. A: Chem. 268 (2007) 82.
[30] M. Choi, D.-H. Lee, K. Na, B.-W. Yu, R. Ryoo, Angew. Chem. Int. Ed. 48 (2009) 3673.
[31] H. Yang, X. Han, G. Li, Y. Wang, Green Chem. 11 (2009) 1184.
[32] S. Jana, S. Haldar, S. Koner, Tetrahedron Lett. 50 (2009) 4820.
[33] A.F. Lee, P.J. Ellis, I.J.S. Fairlamb, K. Wilson, Dalton Trans. 39 (2010) 10473.
[34] D.A. Conlon, B. Pipik, S. Ferdinand, C.R. LeBlond, J.R. Sowa, B. Izzo, P. Collins, G.-J. Ho, J.M. Williams, Y.-J. Shi, Y. Sun, Adv. Synth. Catal. 345 (2003) 931.

[35] S.P. Andrews, A.F. Stepan, H. Tanaka, S.V. Ley, M.D. Smith, Adv. Synth. Catal. 347 (2005) 647.
[36] A.V. Gaikwad, A. Holuigue, M.B. Thathagar, J.E. ten Elshof, G. Rothenberg, Chem. Eur. J. 13 (2007) 6908.
[37] A.K. Diallo, C. Ornelas, L. Salmon, J. Ruiz Aranzaes, D. Astruc, Angew. Chem. Int. Ed. 46 (2007) 8644.
[38] J.-S. Chen, A.N. Vasiliev, A.P. Panarello, J.G. Khinast, Appl. Catal. A: Gen. 325 (2007) 76.
[39] J.M. Richardson, C.W. Jones, J. Catal. 251 (2007) 80.
[40] L. Joucla, G. Cusati, C. Pinel, L. Djakovitch, Appl. Catal. A: Gen. 360 (2009) 145.
[41] J. Demel, M. Lamač, J. Čejka, P. Štěpnička, ChemSusChem 2 (2009) 442.
[42] S.S. Soomro, F.L. Ansari, K. Chatziapostolou, K. Köhler, J. Catal. 273 (2010) 138.
[43] N.T.S. Phan, M. Van Der Sluys, C.W. Jones, Adv. Synth. Catal. 348 (2006) 609.
[44] M.P. Kapoor, W. Fujii, M. Yanagi, Y. Kasama, T. Kimura, H. Nanbu, L.R. Juneja, Micropor. Mesopor. Mater. 116 (2008) 370.
[45] J. Demel, S.-E. Sujandi, J. Park, P. Čejka, Štěpnička, J. Mol. Catal. A: Chem. 302 (2009) 28.
[46] E. Asenath Smith, W. Chen, Langmuir 24 (2008) 12405.
[47] G. Engelhardt, H. Jancke, E. Lippmaa, A. Samoson, J. Organomet. Chem. 210 (1981) 295.
[48] B.N.Z. Dickison, Kristallografiya A88 (1934) 281.
[49] S.D. Kirik, R.F. Mulagaleev, A.I. Blokhin, Acta Crystallogr. C (2004), C60, m449.
[50] C. Röhlich, K. Köhler, Adv. Synth. Catal. 352 (2010) 2263.